Routes to Advanced Laser-Plasma Ion Acceleration

Andrea Macchi

[1]National Institute of Optics, National Research Council (CNR/INO), Pisa, Italy

[2]Department of Physics “Enrico Fermi”, University of Pisa, Italy

ICHEDP 2012, Bejing, October 19, 2012

Main coworkers for this talk

A. Singh Nindrayog[1,2], A. Sgattoni[3,2], M. Tamburini[1,2,*]
T. V.Liseykina[4], P. Londrillo[5], S. Kar[6], M. Borghesi[6],
M. Passoni[3], F. Pegoraro[1,2]

[1]Dipartimento di Fisica “Enrico Fermi”, Università di Pisa, Pisa, Italy
[2]CNR/INO, Pisa, Italy
[3]Dipartimento di Energia, Politecnico di Milano, Milan, Italy
[4]Institut fuer Physik, Universitaet Rostock, Germany
[5]INAF and INFN, Bologna, Italy
[6]Center for Plasma Physics, Queen’s University of Belfast, UK
[*]presently at MPI-K, Heidelberg, Germany

Outline of the talk

A short selection of recent experimental results and of our group's theoretical and simulation work loosely related to such experiments, on the following mechanisms:

- Radiation Pressure Acceleration (RPA)

$\Rightarrow$ exploring "unlimited" RPA in 3D

- Collisional Shock Acceleration (CSA):

$\Rightarrow$ conditions for monoenergetic acceleration

- Target Normal Sheath Acceleration (TNSA):

$\Rightarrow$ enhanced TNSA in foam-covered targets

Outline of the talk

A short selection of recent experimental results and of our group's theoretical and simulation work loosely related to such experiments, on the following mechanisms:

- Radiation Pressure Acceleration (RPA)

$\Rightarrow$ exploring "unlimited" RPA in 3D

- Collisional Shock Acceleration (CSA):

$\Rightarrow$ conditions for monoenergetic acceleration

- Target Normal Sheath Acceleration (TNSA):

$\Rightarrow$ enhanced TNSA in foam-covered targets

Outline of the talk

A short selection of recent experimental results and of our group's theoretical and simulation work loosely related to such experiments, on the following mechanisms:

- Radiation Pressure Acceleration (RPA)

$\Rightarrow$ exploring "unlimited" RPA in 3D

- Collisional Shock Acceleration (CSA):

$\Rightarrow$ conditions for monoenergetic acceleration

- Target Normal Sheath Acceleration (TNSA):

$\Rightarrow$ enhanced TNSA in foam-covered targets

Outline of the talk

A short selection of recent experimental results and of our group's theoretical and simulation work loosely related to such experiments, on the following mechanisms:

- Radiation Pressure Acceleration (RPA)

$\Rightarrow$ exploring "unlimited" RPA in 3D

- Collisional Shock Acceleration (CSA):

$\Rightarrow$ conditions for monoenergetic acceleration

- Target Normal Sheath Acceleration (TNSA):

$\Rightarrow$ enhanced TNSA in foam-covered targets

Reviews of ion acceleration

A. Macchi, M. Borghesi, M. Passoni,
Superintense Laser-Plasma Ion Acceleration,
Rev. Mod. Phys. (2012), submitted.

H. Daido, M. Nishiuchi, A. S. Pirozhkov,
Review of laser-driven ion sources and their applications,
Rep. Prog. Phys. **75**, 056401 (2012).

RPA of thin foils: Light Sail model

$$E_{\text{ion}}(t) \simeq \left(2It/\rho\ell c^2\right)^{1/3} \quad (t \to \infty)$$

$$E_{\text{max}} \simeq m_p c^2 \mathscr{F}^2/(2(\mathscr{F}+1))$$

$$\mathscr{F} = 2(\rho\ell)^{-1}\int_0^\infty I(t')dt' \simeq 2I\tau_p/\rho\ell$$

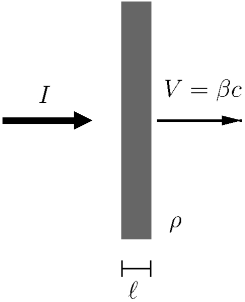

"Dream" features:

Favorable scaling with laser pulse fluence $\mathscr{F}$

100% efficiency in the relativistic limit

"Perfect" monoenergeticity for "rigid" coherent motion of the foil

Limits: "slow" energy gain, foil transparency and deformation

RPA of thin foils: Light Sail model

$$E_{\text{ion}}(t) \simeq \left(2It/\rho\ell c^2\right)^{1/3} \quad (t \to \infty)$$

$$E_{\text{max}} \simeq m_p c^2 \mathscr{F}^2/(2(\mathscr{F}+1))$$

$$\mathscr{F} = 2(\rho\ell)^{-1}\int_0^\infty I(t')dt' \simeq 2I\tau_p/\rho\ell$$

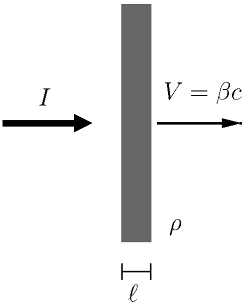

"Dream" features:

Favorable scaling with laser pulse fluence $\mathscr{F}$

100% efficiency in the relativistic limit

"Perfect" monoenergeticity for "rigid" coherent motion of the foil

Limits: "slow" energy gain, foil transparency and deformation

RPA of thin foils: Light Sail model

$$E_{\text{ion}}(t) \simeq \left(2It/\rho\ell c^2\right)^{1/3} \quad (t \to \infty)$$

$$E_{\text{max}} \simeq m_p c^2 \mathscr{F}^2/(2(\mathscr{F}+1))$$

$$\mathscr{F} = 2(\rho\ell)^{-1} \int_0^\infty I(t')dt' \simeq 2I\tau_p/\rho\ell$$

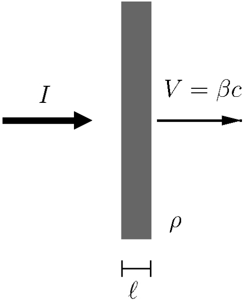

"Dream" features:

Favorable scaling with laser pulse fluence $\mathscr{F}$

100% efficiency in the relativistic limit

"Perfect" monoenergeticity for "rigid" coherent motion of the foil

Limits: "slow" energy gain, foil transparency and deformation

RPA of thin foils: Light Sail model

$$E_{\text{ion}}(t) \simeq \left(2It/\rho\ell c^2\right)^{1/3} \quad (t \to \infty)$$

$$E_{\text{max}} \simeq m_p c^2 \mathscr{F}^2/(2(\mathscr{F}+1))$$

$$\mathscr{F} = 2(\rho\ell)^{-1}\int_0^\infty I(t')dt' \simeq 2I\tau_p/\rho\ell$$

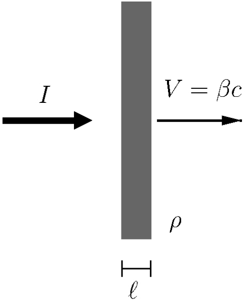

"Dream" features:

Favorable scaling with laser pulse fluence $\mathscr{F}$

100% efficiency in the relativistic limit

"Perfect" monoenergeticity for "rigid" coherent motion of the foil

Limits: "slow" energy gain, foil transparency and deformation

RPA of thin foils: Light Sail model

$$E_{\text{ion}}(t) \simeq \left(2It/\rho\ell c^2\right)^{1/3} \quad (t \to \infty)$$

$$E_{\text{max}} \simeq m_p c^2 \mathscr{F}^2/(2(\mathscr{F}+1))$$

$$\mathscr{F} = 2(\rho\ell)^{-1} \int_0^\infty I(t')dt' \simeq 2I\tau_p/\rho\ell$$

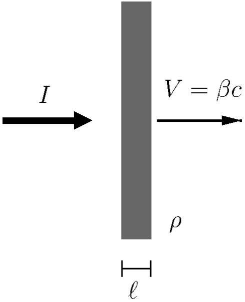

"Dream" features:

Favorable scaling with laser pulse fluence $\mathscr{F}$

100% efficiency in the relativistic limit

"Perfect" monoenergeticity for "rigid" coherent motion of the foil

Limits: "slow" energy gain, foil transparency and deformation

RPA of thin foils: Light Sail model

$$E_{\text{ion}}(t) \simeq \left(2It/\rho\ell c^2\right)^{1/3} \quad (t \to \infty)$$

$$E_{\max} \simeq m_p c^2 \mathscr{F}^2/(2(\mathscr{F}+1))$$

$$\mathscr{F} = 2(\rho\ell)^{-1}\int_0^\infty I(t')dt' \simeq 2I\tau_p/\rho\ell$$

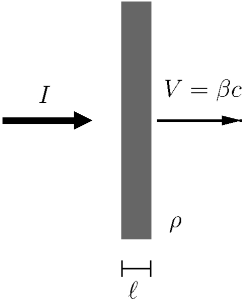

"Dream" features:

Favorable scaling with laser pulse fluence $\mathscr{F}$

100% efficiency in the relativistic limit

"Perfect" monoenergeticity for "rigid" coherent motion of the foil

Limits: "slow" energy gain, foil transparency and deformation

RPA: $\mathscr{F}^2$ scaling observed on VULCAN (RAL, UK)

$\mathscr{E}_{\rm max} \sim \mathscr{F}^2$ (for $\mathscr{F} \ll 1$)

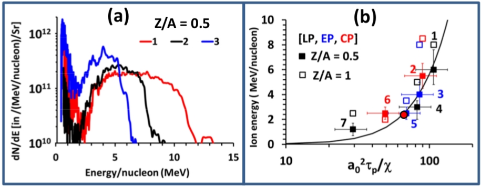

Laser pulse: $t_p \simeq 800\ fs$

3×10^{20} W cm^{-2}

$\sim 10^9$ contrast

Target: $\sim 0.1\ \mu$m metal foil

Multispecies ($Z/A = 1, 1/2$) peak observed with $\Delta\mathscr{E}/\mathscr{E} \simeq 20\%$

Almost no laser polarization dependence observed

S.Kar, K.F.Kakolee, B.Qiao, A.Macchi, M.Borghesi et al.,
Phys. Rev. Lett. (2012), accepted, arXiv:physics/abs/1207.4288

RPA: $\mathscr{F}^2$ scaling observed on VULCAN (RAL, UK)

$\mathscr{E}_{\text{max}} \sim \mathscr{F}^2$ (for $\mathscr{F} \ll 1$)

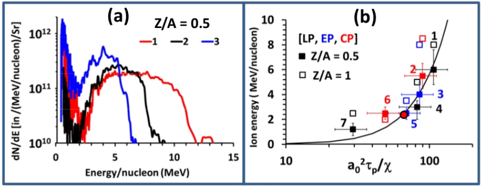

Laser pulse: $t_p \simeq 800\ fs$

3×10^{20} W cm^{-2}

$\sim 10^9$ contrast

Target: $\sim 0.1\ \mu$m metal foil

Multispecies ($Z/A = 1, 1/2$) peak observed with $\Delta\mathscr{E}/\mathscr{E} \simeq 20\%$

Almost no laser polarization dependence observed

S.Kar, K.F.Kakolee, B.Qiao, A.Macchi, M.Borghesi et al.,

Phys. Rev. Lett. (2012), accepted, `arXiv:physics/abs/1207.4288`

RPA: $\mathscr{F}^2$ scaling observed on VULCAN (RAL, UK)

$\mathscr{E}_{\text{max}} \sim \mathscr{F}^2$ (for $\mathscr{F} \ll 1$)

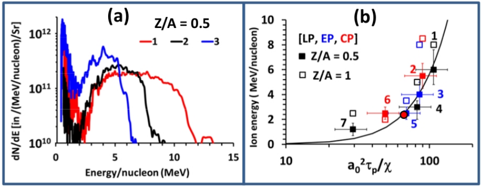

Laser pulse: $t_p \simeq 800\ fs$
3×10^{20} W cm^{-2}
$\sim 10^9$ contrast
Target: $\sim 0.1\ \mu$m metal foil
Multispecies ($Z/A = 1, 1/2$) peak observed with $\Delta\mathscr{E}/\mathscr{E} \simeq 20\%$
Almost no laser polarization dependence observed

S.Kar, K.F.Kakolee, B.Qiao, A.Macchi, M.Borghesi et al.,
Phys. Rev. Lett. (2012), accepted, `arXiv:physics/abs/1207.4288`

RPA: $\mathscr{F}^2$ scaling observed on VULCAN (RAL, UK)

$\mathscr{E}_{\text{max}} \sim \mathscr{F}^2$ (for $\mathscr{F} \ll 1$)

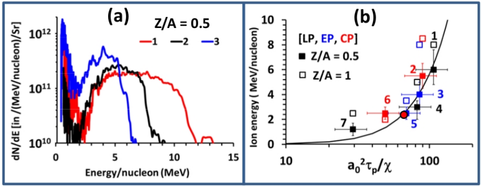

Laser pulse: $t_p \simeq 800\ fs$

3×10^{20} W cm^{-2}

$\sim 10^9$ contrast

Target: $\sim 0.1\ \mu$m metal foil

Multispecies ($Z/A = 1, 1/2$) peak observed with $\Delta\mathscr{E}/\mathscr{E} \simeq 20\%$

Almost no laser polarization dependence observed

S.Kar, K.F.Kakolee, B.Qiao, A.Macchi, M.Borghesi et al.,

Phys. Rev. Lett. (2012), accepted, `arXiv:physics/abs/1207.4288`

Pushing LS forward: “unlimited” acceleration?

Transverse expansion of the target reduces surface density $\rho\ell$
$\Rightarrow$ “unlimited” acceleration possible
at the expense of the number of ions
[Bulanov et al, PRL **104**, 135003 (2010)]
“Faster” gain $E_{\text{ion}}(t) \simeq \left(2It/\rho\ell c^2\right)^{3/5}$ predicted
Route to relativistic (>GeV) ions?

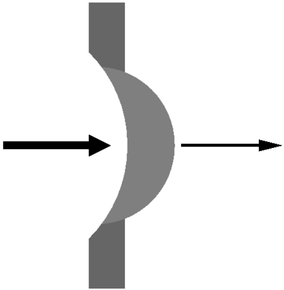

Pushing LS forward: “unlimited” acceleration?

Transverse expansion of the target reduces surface density $\rho\ell$

$\Rightarrow$ “unlimited” acceleration possible
at the expense of the number of ions
[Bulanov et al, PRL **104**, 135003 (2010)]

“Faster” gain $E_{\text{ion}}(t) \simeq \left(2It/\rho\ell c^2\right)^{3/5}$ predicted

Route to relativistic (>GeV) ions?

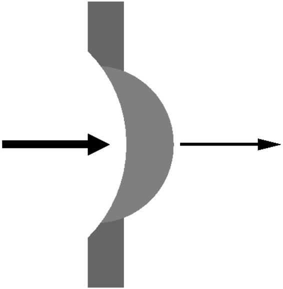

Pushing LS forward: “unlimited” acceleration?

Transverse expansion of the target reduces surface density $\rho\ell$

$\Rightarrow$ “unlimited” acceleration possible at the expense of the number of ions

[Bulanov et al, PRL **104**, 135003 (2010)]

“Faster” gain $E_{\text{ion}}(t) \simeq \left(2It/\rho\ell c^2\right)^{3/5}$ predicted

Route to relativistic (>GeV) ions?

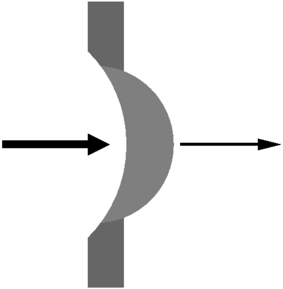

Pushing LS forward: "unlimited" acceleration?

Transverse expansion of the target reduces surface density $\rho\ell$

$\Rightarrow$ "unlimited" acceleration possible at the expense of the number of ions

[Bulanov et al, PRL **104**, 135003 (2010)]

"Faster" gain $E_{\text{ion}}(t) \simeq \left(2It/\rho\ell c^2\right)^{3/5}$ predicted

Route to relativistic (>GeV) ions?

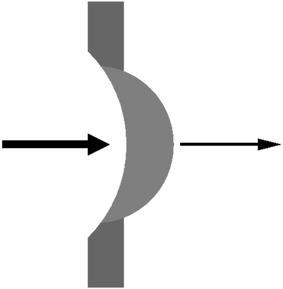

Open issues: polarization, geometry, radiation friction

- Early 3D simulation demonstration of RPA [Esirkepov et al, PRL **92**, 175003 (2004)] at $I > 10^{23}$ W cm^{-2} suggests polarization is inessential
- Unlimited acceleration later demonstrated by 2D simulation and circular polarization (CP) [Bulanov et al, PRL **104**, 135003 (2010)]
- Several studies (after [Macchi et al, PRL **94**, 165003 (2005)]) suggested use of Circular Polarization (CP) for RPA at $I = 10^{18} - 10^{21}$ W cm^{-2}; but also Linear Polarization (LP) may work [Qiao et al, PRL **108**, 115002 (2012)]
- Radiation Friction (RF) important at $I > 10^{23}$ W cm^{-2} ?

$\Rightarrow$ Address polarization, RF and 3D effects in "unlimited" RPA

Open issues: polarization, geometry, radiation friction

- Early 3D simulation demonstration of RPA
  [Esirkepov et al, PRL **92**, 175003 (2004)]
  at $I > 10^{23}$ W cm^{-2} suggests polarization is inessential
- Unlimited acceleration later demonstrated by 2D simulation and circular polarization (CP)
  [Bulanov et al, PRL **104**, 135003 (2010)]
- Several studies (after [Macchi et al, PRL **94**, 165003 (2005)]) suggested use of Circular Polarization (CP) for RPA at $I = 10^{18} - 10^{21}$ W cm^{-2}; but also Linear Polarization (LP) may work [Qiao et al, PRL **108**, 115002 (2012)]
- Radiation Friction (RF) important at $I > 10^{23}$ W cm^{-2} ?

$\Rightarrow$ Address polarization, RF and 3D effects in "unlimited" RPA

Open issues: polarization, geometry, radiation friction

- Early 3D simulation demonstration of RPA [Esirkepov et al, PRL **92**, 175003 (2004)] at $I > 10^{23}$ W cm^{-2} suggests polarization is inessential
- Unlimited acceleration later demonstrated by 2D simulation and circular polarization (CP) [Bulanov et al, PRL **104**, 135003 (2010)]
- Several studies (after [Macchi et al, PRL **94**, 165003 (2005)]) suggested use of Circular Polarization (CP) for RPA at $I = 10^{18} - 10^{21}$ W cm^{-2}; but also Linear Polarization (LP) may work [Qiao et al, PRL **108**, 115002 (2012)]
- Radiation Friction (RF) important at $I > 10^{23}$ W cm^{-2} ?

$\Rightarrow$ Address polarization, RF and 3D effects in "unlimited" RPA

Open issues: polarization, geometry, radiation friction

- Early 3D simulation demonstration of RPA
  [Esirkepov et al, PRL **92**, 175003 (2004)]
  at $I > 10^{23}$ W cm^{-2} suggests polarization is inessential
- Unlimited acceleration later demonstrated by 2D simulation and circular polarization (CP)
  [Bulanov et al, PRL **104**, 135003 (2010)]
- Several studies (after [Macchi et al, PRL **94**, 165003 (2005)]) suggested use of Circular Polarization (CP) for RPA at $I = 10^{18} - 10^{21}$ W cm^{-2}; but also Linear Polarization (LP) may work [Qiao et al, PRL **108**, 115002 (2012)]
- Radiation Friction (RF) important at $I > 10^{23}$ W cm^{-2} ?

$\Rightarrow$ Address polarization, RF and 3D effects in “unlimited” RPA

Open issues: polarization, geometry, radiation friction

- Early 3D simulation demonstration of RPA [Esirkepov et al, PRL **92**, 175003 (2004)] at $I > 10^{23}$ W cm^{-2} suggests polarization is inessential
- Unlimited acceleration later demonstrated by 2D simulation and circular polarization (CP) [Bulanov et al, PRL **104**, 135003 (2010)]
- Several studies (after [Macchi et al, PRL **94**, 165003 (2005)]) suggested use of Circular Polarization (CP) for RPA at $I = 10^{18} - 10^{21}$ W cm^{-2}; but also Linear Polarization (LP) may work [Qiao et al, PRL **108**, 115002 (2012)]
- Radiation Friction (RF) important at $I > 10^{23}$ W cm^{-2} ?

$\Rightarrow$ Address polarization, RF and 3D effects in “unlimited” RPA

Set-up of 3D RPA simulations

- Laser pulse: $(9T) \times (10\lambda)^2$ (FWHM) [$T = \lambda/c$]
  $\sin^2 \times$Gaussian shape, $a_0 = 280$ (198) for LP (CP),
  $\lambda = 0.8$ μm ($I = 1.7 \times 10^{23}$ W cm^{-2})
- Plasma: $\ell = 1\lambda$, $n_0 = 64n_c$, $Z = A = 1$

  Note: $a_0 \simeq \zeta = \pi(n_e/n_c)(\ell/\lambda)$
- RF included via Landau-Lifshitz force
- Numerical: $1320 \times 896 \times 896$ grid, $\Delta x = \Delta y = \Delta z = \lambda/44$,
  $\Delta t = T/80 = \lambda/80c$, 216 particles per cell (for both e and p),
  1.526×10^{10} in total

Runs performed on 1024 processors (1.7 GBytes each) of IBM-SP6 at CINECA (Italy)

Set-up of 3D RPA simulations

- Laser pulse: $(9T) \times (10\lambda)^2$ (FWHM) $[T = \lambda/c]$
  $\sin^2 \times$Gaussian shape, $a_0 = 280$ (198) for LP (CP),
  $\lambda = 0.8$ μm ($I = 1.7 \times 10^{23}$ W cm^{-2})
- Plasma: $\ell = 1\lambda$, $n_0 = 64n_c$, $Z = A = 1$

  Note: $a_0 \simeq \zeta = \pi(n_e/n_c)(\ell/\lambda)$
- RF included via Landau-Lifshitz force
- Numerical: $1320 \times 896 \times 896$ grid, $\Delta x = \Delta y = \Delta z = \lambda/44$,
  $\Delta t = T/80 = \lambda/80c$, 216 particles per cell (for both e and p),
  1.526×10^{10} in total

Runs performed on 1024 processors (1.7 GBytes each) of IBM-SP6 at CINECA (Italy)

Set-up of 3D RPA simulations

- Laser pulse: $(9T) \times (10\lambda)^2$ (FWHM) $[T = \lambda/c]$
  $\sin^2 \times$Gaussian shape, $a_0 = 280$ (198) for LP (CP),
  $\lambda = 0.8$ μm ($I = 1.7 \times 10^{23}$ W cm^{-2})
- Plasma: $\ell = 1\lambda$, $n_0 = 64n_c$, $Z = A = 1$
  Note: $a_0 \simeq \zeta = \pi(n_e/n_c)(\ell/\lambda)$
- RF included via Landau-Lifshitz force
- Numerical: $1320 \times 896 \times 896$ grid, $\Delta x = \Delta y = \Delta z = \lambda/44$,
  $\Delta t = T/80 = \lambda/80c$, 216 particles per cell (for both e and p),
  1.526×10^{10} in total

Runs performed on 1024 processors (1.7 GBytes each) of IBM-SP6 at CINECA (Italy)

Set-up of 3D RPA simulations

- Laser pulse: $(9T) \times (10\lambda)^2$ (FWHM) [$T = \lambda/c$]
  $\sin^2 \times$Gaussian shape, $a_0 = 280$ (198) for LP (CP),
  $\lambda = 0.8$ μm ($I = 1.7 \times 10^{23}$ W cm^{-2})
- Plasma: $\ell = 1\lambda$, $n_0 = 64 n_c$, $Z = A = 1$

  Note: $a_0 \simeq \zeta = \pi(n_e/n_c)(\ell/\lambda)$
- RF included via Landau-Lifshitz force
- Numerical: $1320 \times 896 \times 896$ grid, $\Delta x = \Delta y = \Delta z = \lambda/44$,
  $\Delta t = T/80 = \lambda/80c$, 216 particles per cell (for both e and p),
  1.526×10^{10} in total

Runs performed on 1024 processors (1.7 GBytes each) of IBM-SP6 at CINECA (Italy)

Set-up of 3D RPA simulations

- Laser pulse: $(9T) \times (10\lambda)^2$ (FWHM) [$T = \lambda/c$]
  $\sin^2 \times$Gaussian shape, $a_0 = 280$ (198) for LP (CP),
  $\lambda = 0.8$ μm ($I = 1.7 \times 10^{23}$ W cm^{-2})
- Plasma: $\ell = 1\lambda$, $n_0 = 64n_c$, $Z = A = 1$
  Note: $a_0 \simeq \zeta = \pi(n_e/n_c)(\ell/\lambda)$
- RF included via Landau-Lifshitz force
- Numerical: $1320 \times 896 \times 896$ grid, $\Delta x = \Delta y = \Delta z = \lambda/44$,
  $\Delta t = T/80 = \lambda/80c$, 216 particles per cell (for both e and p),
  1.526×10^{10} in total

Runs performed on 1024 processors (1.7 GBytes each) of IBM-SP6 at CINECA (Italy)

Set-up of 3D RPA simulations

- Laser pulse: $(9T) \times (10\lambda)^2$ (FWHM) [$T = \lambda/c$]
  $\sin^2 \times$Gaussian shape, $a_0 = 280\ (198)$ for LP (CP),
  $\lambda = 0.8\ \mu$m ($I = 1.7 \times 10^{23}$ W cm^{-2})
- Plasma: $\ell = 1\lambda$, $n_0 = 64 n_c$, $Z = A = 1$
  Note: $a_0 \simeq \zeta = \pi(n_e/n_c)(\ell/\lambda)$
- RF included via Landau-Lifshitz force
- Numerical: $1320 \times 896 \times 896$ grid, $\Delta x = \Delta y = \Delta z = \lambda/44$,
  $\Delta t = T/80 = \lambda/80c$, 216 particles per cell (for both e and p),
  1.526×10^{10} in total

Runs performed on 1024 processors (1.7 GBytes each) of IBM-SP6 at CINECA (Italy)

Space-energy distribution in 3D simulations

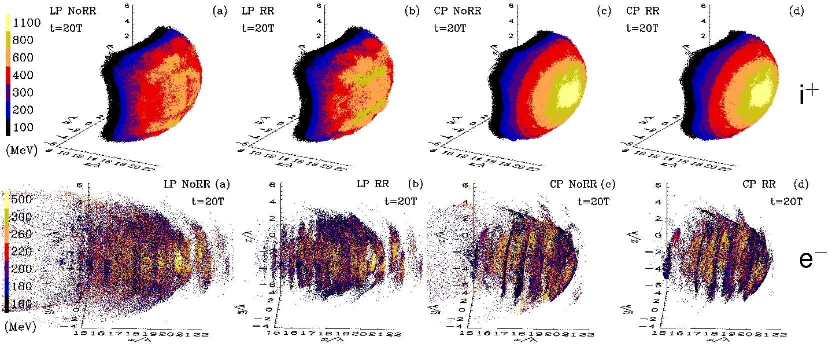

CP: symmetric, collimated ion distribution, weak RF effects

LP: asymmetric two-lobe ion distribution, strong RF effects

[Tamburini, Liseykina, Pegoraro, Macchi, PRE **85**, 016407 (2012)]

Space-energy distribution in 3D simulations

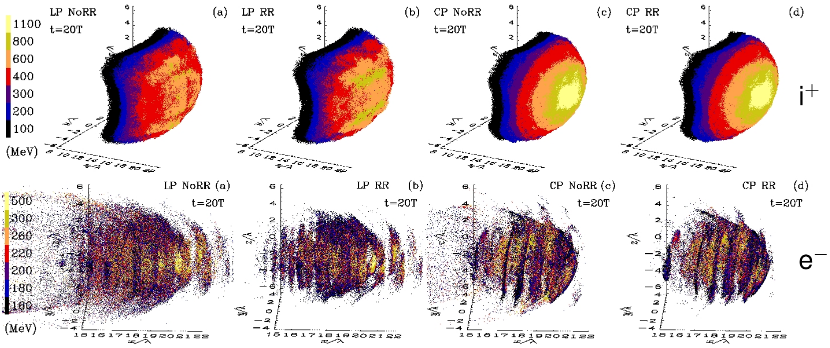

CP: symmetric, collimated ion distribution, weak RF effects

LP: asymmetric two-lobe ion distribution, strong RF effects

[Tamburini, Liseykina, Pegoraro, Macchi, PRE **85**, 016407 (2012)]

Space-energy distribution in 3D simulations

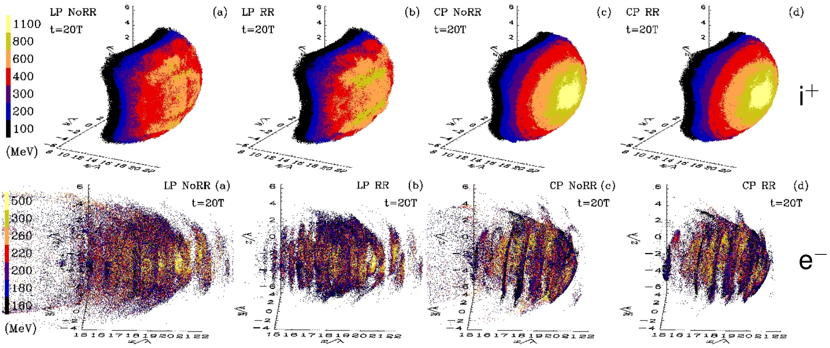

CP: symmetric, collimated ion distribution, weak RF effects

LP: asymmetric two-lobe ion distribution, strong RF effects

[Tamburini, Liseykina, Pegoraro, Macchi, PRE **85**, 016407 (2012)]

Pulse self-wrapping by the foil

Sections of 3D fields [a1)-d3)] vs 2D simulations [e)-f)]

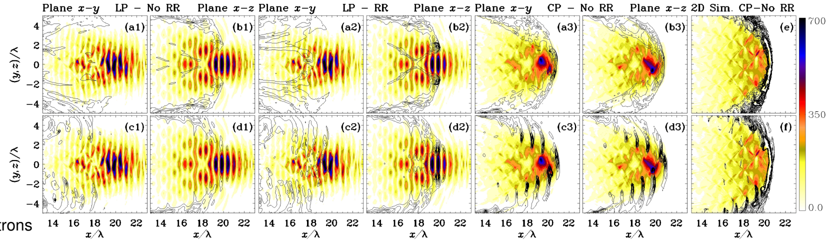

Focusing of the pulse down to $\sim \lambda^3$ volume for CP [see series -3)]

"Wrapping" and focusing effects are weaker in 2D vs 3D [see e)-f)]

Breakthrough in the foil occurs for LP [see series -1)-2)]

Pulse self-wrapping by the foil

Sections of 3D fields [a1)-d3)] vs 2D simulations [e)-f)]

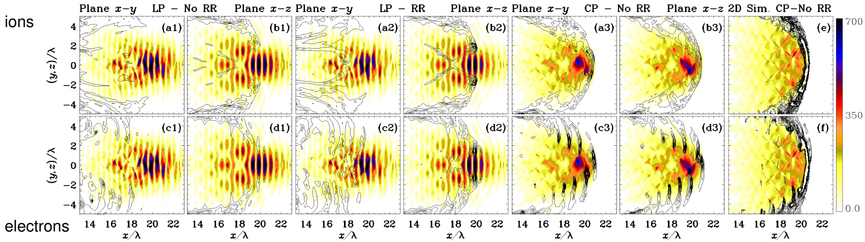

- Focusing of the pulse down to $\sim \lambda^3$ volume for CP [see series -3)]
- "Wrapping" and focusing effects are weaker in 2D vs 3D [see e)-f)]
- Breakthrough in the foil occurs for LP [see series -1)-2)]

Pulse self-wrapping by the foil

Sections of 3D fields [a1)-d3)] vs 2D simulations [e)-f)]

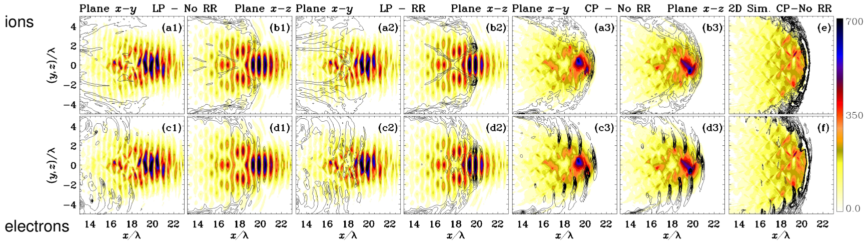

Focusing of the pulse down to $\sim \lambda^3$ volume for CP [see series -3)]

“Wrapping” and focusing effects are weaker in 2D vs 3D [see e)-f)]

Breakthrough in the foil occurs for LP [see series -1)-2)]

Pulse self-wrapping by the foil

Sections of 3D fields [a1)-d3)] vs 2D simulations [e)-f)]

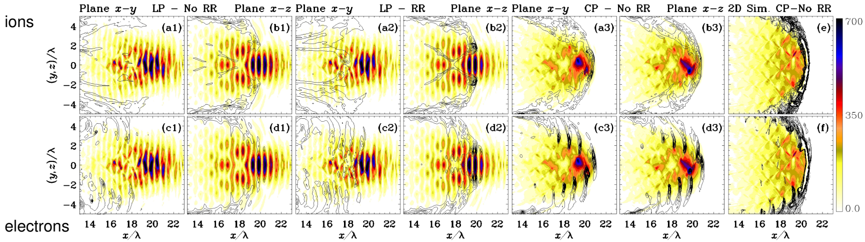

Focusing of the pulse down to $\sim \lambda^3$ volume for CP [see series -3)]

“Wrapping” and focusing effects are weaker in 2D vs 3D [see e)-f)]

Breakthrough in the foil occurs for LP [see series -1)-2)]

Pulse self-wrapping by the foil

Sections of 3D fields [a1)-d3)] vs 2D simulations [e)-f)]

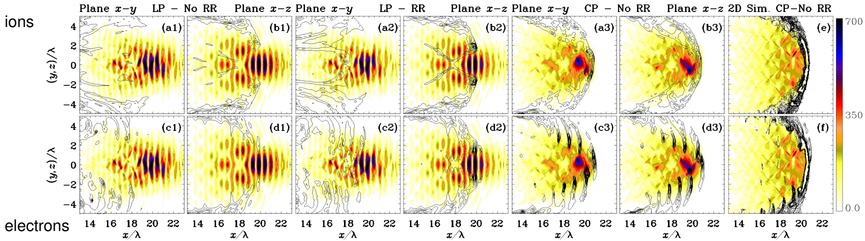

Focusing of the pulse down to $\sim \lambda^3$ volume for CP [see series -3)]

"Wrapping" and focusing effects are weaker in 2D vs 3D [see e)-f)]

Breakthrough in the foil occurs for LP [see series -1)-2)]

Effects of reduced dimensionality and resolution

Comparison of 3D ion spectra with 2D results (both S and P for LP) for both the same and higher resolution

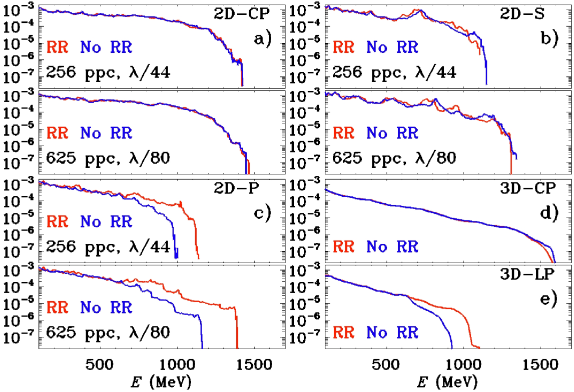

Effects of 2D vs 3D and of limited resolution are evident, but kept below physical effects

The “optimal” CP case is the most robust (but energy is *lower* in 2D vs 3D !)

Effects of reduced dimensionality and resolution

Comparison of 3D ion spectra with 2D results (both S and P for LP) for both the same and higher resolution

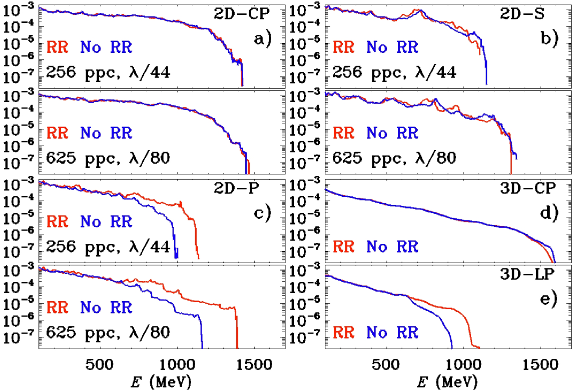

Effects of 2D vs 3D and of limited resolution are evident, but kept below physical effects

The "optimal" CP case is the most robust (but energy is *lower* in 2D vs 3D !)

Effects of reduced dimensionality and resolution

Comparison of 3D ion spectra with 2D results (both S and P for LP) for both the same and higher resolution

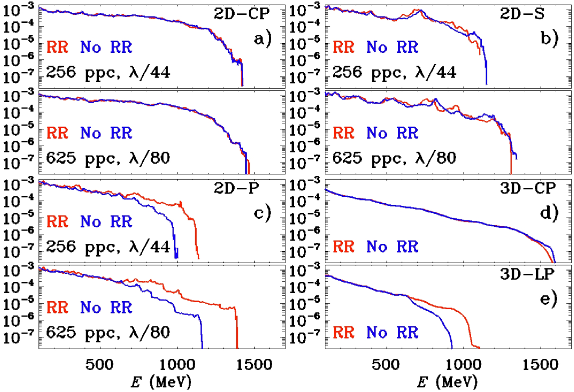

Effects of 2D vs 3D and of limited resolution are evident, but kept below physical effects

The "optimal" CP case is the most robust (but energy is *lower* in 2D vs 3D !)

Effects of reduced dimensionality and resolution

Comparison of 3D ion spectra with 2D results (both S and P for LP) for both the same and higher resolution

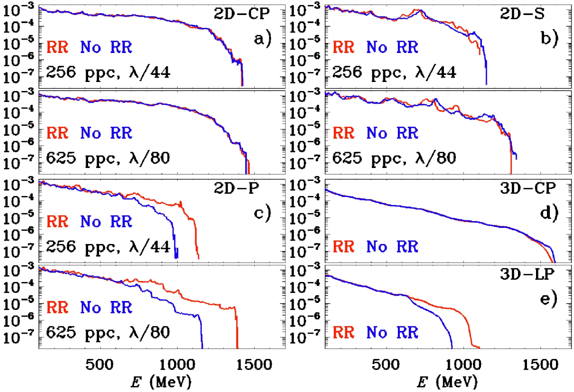

Effects of 2D vs 3D and of limited resolution are evident, but kept below physical effects

The “optimal” CP case is the most robust (but energy is *lower* in 2D vs 3D !)

Unlimited acceleration confirmed (and enforced?)

- For CP: the energy cut-off corresponds to ions on axis and is *higher* in 3D than in 2D/1D

  1: more efficient rarefaction by transverse expansion

  2: increase of energy density on axis by pulse self-wrapping
- CP optimizes ion acceleration (collimated distribution, negligible RR effects) with respect to LP
- Breaking of the pulse through the foil destroys RPA
- Notice, however, that in the transparency regime high-energy ions have been observed (B.M.Hegelich and LANL team)

Unlimited acceleration confirmed (and enforced?)

- For CP: the energy cut-off corresponds to ions on axis and is *higher* in 3D than in 2D/1D

  1: more efficient rarefaction by transverse expansion

  2: increase of energy density on axis by pulse self-wrapping
- CP optimizes ion acceleration (collimated distribution, negliglible RR effects) with respect to LP
- Breaking of the pulse through the foil destroys RPA
- Notice, however, that in the transparency regime high-energy ions have been observed (B.M.Hegelich and LANL team)

Unlimited acceleration confirmed (and enforced?)

- For CP: the energy cut-off corresponds to ions on axis and is *higher* in 3D than in 2D/1D

  1: more efficient rarefaction by transverse expansion

  2: increase of energy density on axis by pulse self-wrapping
- CP optimizes ion acceleration (collimated distribution, negligible RR effects) with respect to LP
- Breaking of the pulse through the foil destroys RPA

- Notice, however, that in the transparency regime high-energy ions have been observed (B.M.Hegelich and LANL team)

Unlimited acceleration confirmed (and enforced?)

- For CP: the energy cut-off corresponds to ions on axis and is *higher* in 3D than in 2D/1D

  1: more efficient rarefaction by transverse expansion

  2: increase of energy density on axis by pulse self-wrapping
- CP optimizes ion acceleration (collimated distribution, negligible RR effects) with respect to LP
- Breaking of the pulse through the foil destroys RPA
- Notice, however, that in the transparency regime high-energy ions have been observed (B.M.Hegelich and LANL team)

Unlimited acceleration confirmed (and enforced?)

- For CP: the energy cut-off corresponds to ions on axis and is *higher* in 3D than in 2D/1D

  1: more efficient rarefaction by transverse expansion

  2: increase of energy density on axis by pulse self-wrapping
- CP optimizes ion acceleration (collimated distribution, negligible RR effects) with respect to LP
- Breaking of the pulse through the foil destroys RPA
- Notice, however, that in the transparency regime high-energy ions have been observed (B.M.Hegelich and LANL team)

Unlimited acceleration confirmed (and enforced?)

- For CP: the energy cut-off corresponds to ions on axis and is *higher* in 3D than in 2D/1D

  1: more efficient rarefaction by transverse expansion

  2: increase of energy density on axis by pulse self-wrapping
- CP optimizes ion acceleration (collimated distribution, negligible RR effects) with respect to LP
- Breaking of the pulse through the foil destroys RPA
- Notice, however, that in the transparency regime high-energy ions have been observed (B.M.Hegelich and LANL team)

Unlimited acceleration confirmed (and enforced?)

- For CP: the energy cut-off corresponds to ions on axis and is *higher* in 3D than in 2D/1D

  1: more efficient rarefaction by transverse expansion

  2: increase of energy density on axis by pulse self-wrapping
- CP optimizes ion acceleration (collimated distribution, negligible RR effects) with respect to LP
- Breaking of the pulse through the foil destroys RPA
- Notice, however, that in the transparency regime high-energy ions have been observed (B.M.Hegelich and LANL team)

Collisionless Shock Acceleration

- Basic idea: a Collisionless Shock Wave of velocity $v_s = Mc_s$ with $M > 1$ ($c_s = \sqrt{ZT_e/Am_p}$) is driven into an overdense plasma by either piston-like push of radiation pressure or "suprathermal" pressure of fast electrons
- Ion acceleration occurs in the plasma bulk by *reflection* from the shock front: $v_i \simeq 2v_s$ ("moving wall" reflection)
- Reflected ions are *monoenergetic* if v_s is constant and have multi–MeV energy if $T_e \simeq m_e c^2 \left(\sqrt{1+a_0^2/2}-1\right)$ (*fast* electron temperature)

Collisionless Shock Acceleration

- Basic idea: a Collisionless Shock Wave of velocity $\upsilon_s = Mc_s$ with $M > 1$ ($c_s = \sqrt{ZT_e/Am_p}$) is driven into an overdense plasma by either piston-like push of radiation pressure or "suprathermal" pressure of fast electrons
- Ion acceleration occurs in the plasma bulk by *reflection* from the shock front: $\upsilon_i \simeq 2\upsilon_s$ ("moving wall" reflection)
- Reflected ions are *monoenergetic* if υ_s is constant and have multi–MeV energy if $T_e \simeq m_e c^2 \left(\sqrt{1+a_0^2/2}-1\right)$ (*fast* electron temperature)

Collisionless Shock Acceleration

- Basic idea: a Collisionless Shock Wave of velocity $v_s = Mc_s$ with $M > 1$ ($c_s = \sqrt{ZT_e/Am_p}$) is driven into an overdense plasma by either piston-like push of radiation pressure or "suprathermal" pressure of fast electrons
- Ion acceleration occurs in the plasma bulk by *reflection* from the shock front: $v_i \simeq 2v_s$ ("moving wall" reflection)
- Reflected ions are *monoenergetic* if v_s is constant and have multi–MeV energy if $T_e \simeq m_e c^2 \left(\sqrt{1 + a_0^2/2} - 1\right)$ (*fast* electron temperature)

Monoenergetic protons from CO_2 laser-gas interaction

[Haberberger et al, Nat. Phys. **8**, 95 (2012)]

Laser: $\lambda = 10\ \mu$m
$I = 6.5 \times 10^{16}$ W cm^{-2}
modulated 100 ps train of 3 ps pulses

Target: H_2 jet, $n_0 \leq \times 4 \times 10^{19}$ cm^{-3}

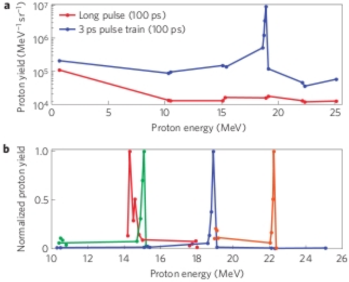

Figure 2 | Proton energy spectra. a, Proton spectra obtained with a 100-ps-long laser pulse (red) and a 100 ps macropulse consisting of a number of 3 ps micropulses (blue) both containing 60 J. The typical noise level on a single CR39 detector was 100 pits. The total number of protons contained within the monoenergetic peak was 2.5×10^5. **b**, The details of the energy spectra on four different laser shots with different macropulse structures (number of pulses and a_0 values ranging from 1.5 to 2.5).

Very peaked spectra at $\sim$20 MeV but with low number of ions

Is efficiency of CSA not compatible with monoenergeticity?

Monoenergetic protons from CO_2 laser-gas interaction

[Haberberger et al,
Nat. Phys. **8**, 95 (2012)]

Laser: $\lambda = 10\ \mu$m
$I = 6.5 \times 10^{16}$ W cm^{-2}
modulated 100 ps train
of 3 ps pulses
Target: H_2 jet, $n_0 \leq \times 4 \times 10^{19}$ cm^{-3}

Very peaked spectra at ∼20 MeV
but with low number of ions

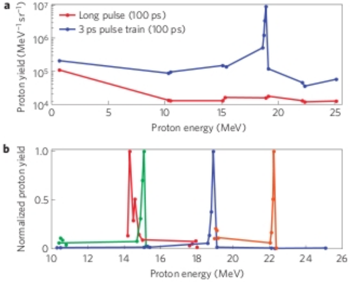

Figure 2 | Proton energy spectra. a, Proton spectra obtained with a 100-ps-long laser pulse (red) and a 100 ps macropulse consisting of a number of 3 ps micropulses (blue) both containing 60 J. The typical noise level on a single CR39 detector was 100 pits. The total number of protons contained within the monoenergetic peak was 2.5×10^5. **b**, The details of the energy spectra on four different laser shots with different macropulse structures (number of pulses and a_0 values ranging from 1.5 to 2.5).

Is efficiency of CSA not compatible with monoenergeticity?

Monoenergetic protons from CO_2 laser-gas interaction

[Haberberger et al,
Nat. Phys. **8**, 95 (2012)]
Laser: $\lambda = 10\ \mu$m
$I = 6.5 \times 10^{16}$ W cm^{-2}
modulated 100 ps train
of 3 ps pulses
Target: H_2 jet, $n_0 \leq \times 4 \times 10^{19}$ cm^{-3}

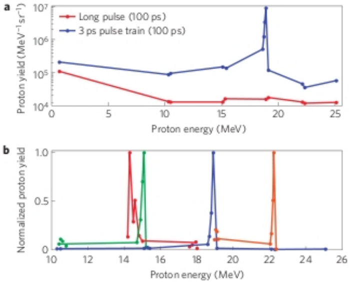

Figure 2 | Proton energy spectra. a, Proton spectra obtained with a 100-ps-long laser pulse (red) and a 100 ps macropulse consisting of a number of 3 ps micropulses (blue) both containing 60 J. The typical noise level on a single CR39 detector was 100 pits. The total number of protons contained within the monoenergetic peak was 2.5×10^5. **b**, The details of the energy spectra on four different laser shots with different macropulse structures (number of pulses and a_0 values ranging from 1.5 to 2.5).

Very peaked spectra at $\sim$20 MeV
but with low number of ions

Is efficiency of CSA not compatible with monoenergeticity?

Monoenergetic protons from CO_2 laser-gas interaction

[Haberberger et al,
Nat. Phys. **8**, 95 (2012)]

Laser: $\lambda = 10\ \mu$m

$I = 6.5 \times 10^{16}$ W cm^{-2}

modulated 100 ps train of 3 ps pulses

Target: H_2 jet, $n_0 \leq \times 4 \times 10^{19}$ cm^{-3}

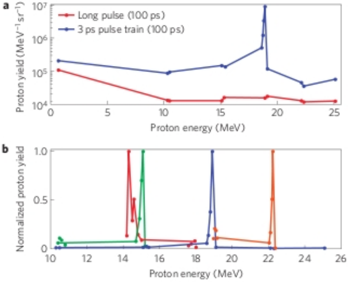

Figure 2 | Proton energy spectra. a, Proton spectra obtained with a 100-ps-long laser pulse (red) and a 100 ps macropulse consisting of a number of 3 ps micropulses (blue) both containing 60 J. The typical noise level on a single CR39 detector was 100 pits. The total number of protons contained within the monoenergetic peak was 2.5×10^5. **b**, The details of the energy spectra on four different laser shots with different macropulse structures (number of pulses and a_0 values ranging from 1.5 to 2.5).

Very peaked spectra at $\sim$20 MeV
but with low number of ions

Is efficiency of CSA not compatible with monoenergeticity?

More on CO_2 experiments: CSA or RPA?

Monoenergetic acceleration
[Palmer et al, PRL **106**, 14801 (2011)]
attributed to a
"radiation pressure driven shock"
using *circular* polarization

But no CSA in the bulk is observed
using CP since $T_e \simeq 0$; mechanism
may be "hole boring" ("piston") RPA
[Macchi et al, PRL **94**, 165003 (2005);
Macchi, Nindrayog, Pegoraro,
PRE **85**, 046402 (2012)]

More on CO_2 experiments: CSA or RPA?

Monoenergetic acceleration
[Palmer et al, PRL **106**, 14801 (2011)]
attributed to a
"radiation pressure driven shock"
using *circular* polarization

But no CSA in the bulk is observed using CP since $T_e \simeq 0$; mechanism may be "hole boring" ("piston") RPA
[Macchi et al, PRL **94**, 165003 (2005);
Macchi, Nindrayog, Pegoraro,
PRE **85**, 046402 (2012)]

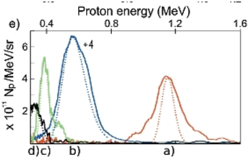

FIG. 1 (color online). Raw and processed proton spectra for varying peak density n and vacuum intensity I showing scaling of peak proton energy $E_{max} \propto I/nc$ [MeV]. Parameter I/n shown to the right of the respective raw images. Shots taken with (a) $I = 6.4$, $n = 6.1n_{cr}$, (b) $I = 5.5$, $n = 6.1n_{cr}$, (c) $I = 5.9$, $n = 7.6n_{cr}$, (d) $I = 5.7$, $n = 8.0n_{cr}$ (I in units of 10^{15} W cm^{-2}). (e) Background subtracted (solid lines) and also corrected (dashed lines) spectra. Heights of corrected spectra adjusted to match those of raw lineouts. Lineout corresponding to (b) reduced 4× to fit on the same scale.

More on CO_2 experiments: CSA or RPA?

Monoenergetic acceleration
[Palmer et al, PRL **106**, 14801 (2011)]
attributed to a
“radiation pressure driven shock”
using *circular* polarization

But no CSA in the bulk is observed
using CP since $T_e \simeq 0$; mechanism
may be “hole boring” (“piston”) RPA
[Macchi et al, PRL **94**, 165003 (2005);
Macchi, Nindrayog, Pegoraro,
PRE **85**, 046402 (2012)]

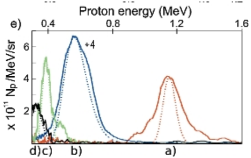

FIG. 1 (color online). Raw and processed proton spectra for varying peak density n and vacuum intensity I showing scaling of peak proton energy $E_{max} \propto I/nc$ [MeV]. Parameter I/n shown to the right of the respective raw images. Shots taken with (a) $I = 6.4$, $n = 6.1n_{cr}$, (b) $I = 5.5$, $n = 6.1n_{cr}$, (c) $I = 5.9$, $n = 7.6n_{cr}$, (d) $I = 5.7$, $n = 8.0n_{cr}$ (I in units of 10^{15} W cm^{-2}). (e) Background subtracted (solid lines) and also corrected (dashed lines) spectra. Heights of corrected spectra adjusted to match those of raw lineouts. Lineout corresponding to (b) reduced 4× to fit on the same scale.

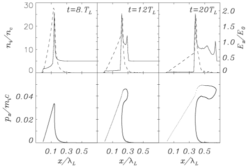

Hints from Collisionless Shocks theory

[Tidman & Krall, *Shock Waves in Collisionless Plasmas* (Wiley, 1971)]

- Ion reflection may *not* form at all in the absence of reflected ions
- Background ions *must* have some energy spread otherwise they would *all* either reflected or not
- Reflected ions are on the tail of the ion distribution ($v_i > v_s - \sqrt{2e\Phi_M/m_i}$ with Φ_M shock potential barrier)
- Too many ions reflected may lead to shock loading

$\Rightarrow$ shock front slows down and monoenergeticity is lost

- Optimize ion temperature T_i
  for energy spread vs. number of ions

Hints from Collisionless Shocks theory

[Tidman & Krall, *Shock Waves in Collisionless Plasmas* (Wiley, 1971)]

- Ion reflection may *not* form at all in the absence of reflected ions
- Background ions *must* have some energy spread otherwise they would *all* either reflected or not
- Reflected ions are on the tail of the ion distribution ($v_i > v_s - \sqrt{2e\Phi_M/m_i}$ with Φ_M shock potential barrier)
- Too many ions reflected may lead to shock loading

$\Rightarrow$ shock front slows down and monoenergeticity is lost

- Optimize ion temperature T_i
  for energy spread vs. number of ions

Hints from Collisionless Shocks theory

[Tidman & Krall, *Shock Waves in Collisionless Plasmas* (Wiley, 1971)]

- Ion reflection may *not* form at all in the absence of reflected ions
- Background ions *must* have some energy spread otherwise they would *all* either reflected or not
- Reflected ions are on the tail of the ion distribution ($v_i > v_s - \sqrt{2e\Phi_{\mathrm{M}}/m_i}$ with Φ_{M} shock potential barrier)
- Too many ions reflected may lead to shock loading

$\Rightarrow$ shock front slows down and monoenergeticity is lost

- Optimize ion temperature T_i for energy spread vs. number of ions

Hints from Collisionless Shocks theory

[Tidman & Krall, *Shock Waves in Collisionless Plasmas* (Wiley, 1971)]

- Ion reflection may *not* form at all in the absence of reflected ions
- Background ions *must* have some energy spread otherwise they would *all* either reflected or not
- Reflected ions are on the tail of the ion distribution ($v_i > v_s - \sqrt{2e\Phi_{\mathrm{M}}/m_i}$ with Φ_{M} shock potential barrier)
- Too many ions reflected may lead to shock loading

$\Rightarrow$ shock front slows down and monoenergeticity is lost

- Optimize ion temperature T_i
  for energy spread vs. number of ions

Hints from Collisionless Shocks theory

[Tidman & Krall, *Shock Waves in Collisionless Plasmas* (Wiley, 1971)]

- Ion reflection may *not* form at all in the absence of reflected ions
- Background ions *must* have some energy spread otherwise they would *all* either reflected or not
- Reflected ions are on the tail of the ion distribution ($v_i > v_s - \sqrt{2e\Phi_M/m_i}$ with Φ_M shock potential barrier)
- Too many ions reflected may lead to shock loading

$\Rightarrow$ shock front slows down and monoenergeticity is lost

- Optimize ion temperature T_i
  for energy spread vs. number of ions

Hints from Collisionless Shocks theory

[Tidman & Krall, *Shock Waves in Collisionless Plasmas* (Wiley, 1971)]

- Ion reflection may *not* form at all in the absence of reflected ions
- Background ions *must* have some energy spread otherwise they would *all* either reflected or not
- Reflected ions are on the tail of the ion distribution ($v_i > v_s - \sqrt{2e\Phi_{\mathrm{M}}/m_i}$ with Φ_{M} shock potential barrier)
- Too many ions reflected may lead to shock loading

$\Rightarrow$ shock front slows down and monoenergeticity is lost

- Optimize ion temperature T_i for energy spread vs. number of ions

Hints from Collisionless Shocks theory

[Tidman & Krall, *Shock Waves in Collisionless Plasmas* (Wiley, 1971)]

- Ion reflection may *not* form at all in the absence of reflected ions
- Background ions *must* have some energy spread otherwise they would *all* either reflected or not
- Reflected ions are on the tail of the ion distribution ($v_i > v_s - \sqrt{2e\Phi_\text{M}/m_i}$ with Φ_M shock potential barrier)
- Too many ions reflected may lead to shock loading

$\Rightarrow$ shock front slows down and monoenergeticity is lost

- Optimize ion temperature T_i for energy spread vs. number of ions

CSA with warm ions: 1D simulation - I

Parameters:

$a_0 = 1$

$\tau_p = 4T = 4\lambda/c$

$n_e = 2n_c$

$T_i = 100$ eV

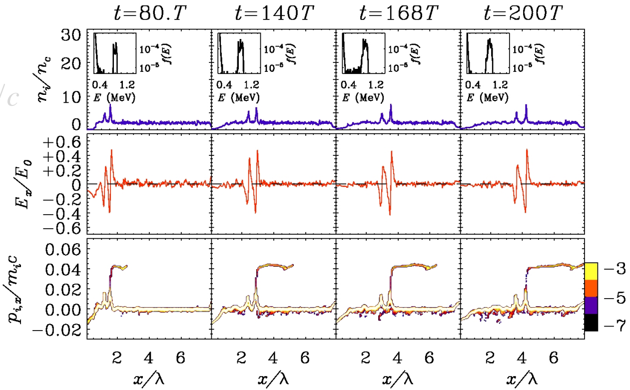

Steady ion reflection produces a narrow energy spectrum

CSA with warm ions: 1D simulation - I

Parameters:

$a_0 = 1$

$\tau_p = 4T = 4\lambda/c$

$n_e = 2n_c$

$T_i = 100$ eV

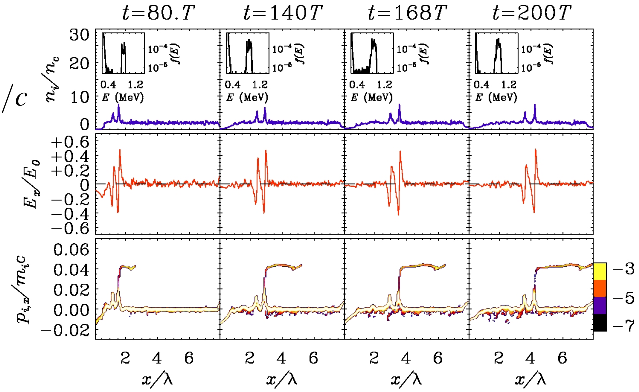

Steady ion reflection produces a narrow energy spectrum

CSA with warm ions: 1D simulation - I

Parameters:

$a_0 = 1$

$\tau_p = 4T = 4\lambda/c$

$n_e = 2n_c$

$T_i = 100$ eV

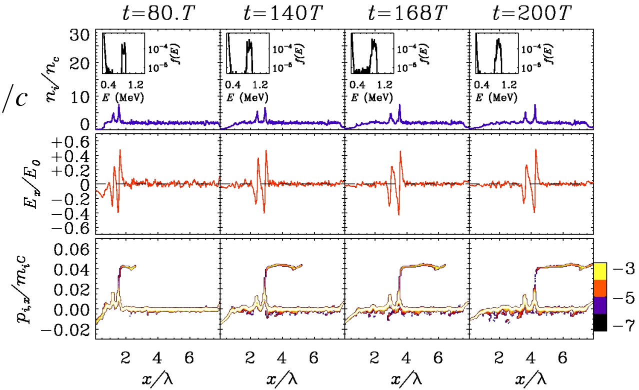

Steady ion reflection produces a narrow energy spectrum

CSA with warm ions: 1D simulation - II

Parameters:

$a_0 = 16$

$\tau_p = 4T = 4\lambda/c$

$n_e = 20n_c$

$T_i = 1$ keV

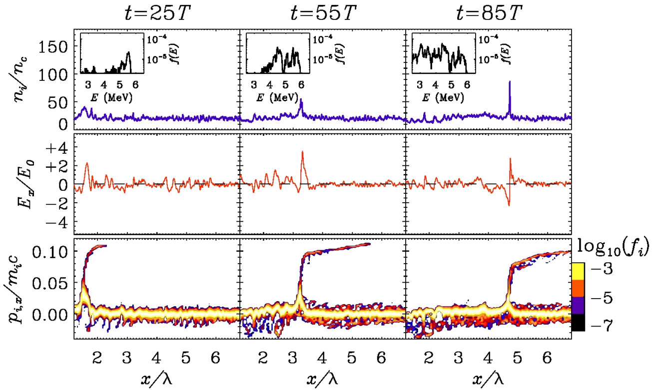

Too high T_i causes shock to slow down and spectrum to broaden

CSA with warm ions: 1D simulation - II

Parameters:

$a_0 = 16$

$\tau_p = 4T = 4\lambda/c$

$n_e = 20n_c$

$T_i = 1$ keV

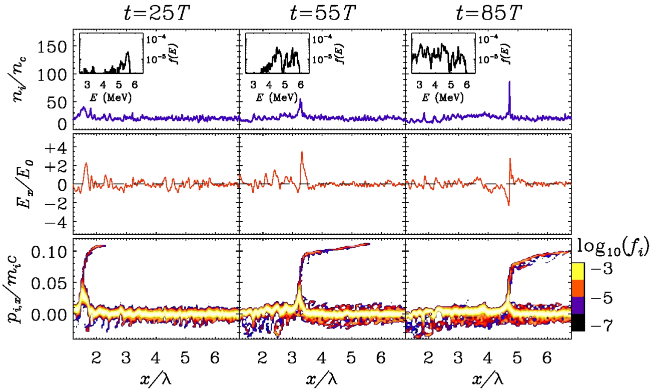

Too high T_i causes shock to slow down and spectrum to broaden

CSA with warm ions: 1D simulation - II

Parameters:

$a_0 = 16$

$\tau_p = 4T = 4\lambda/c$

$n_e = 20n_c$

$T_i = 1$ keV

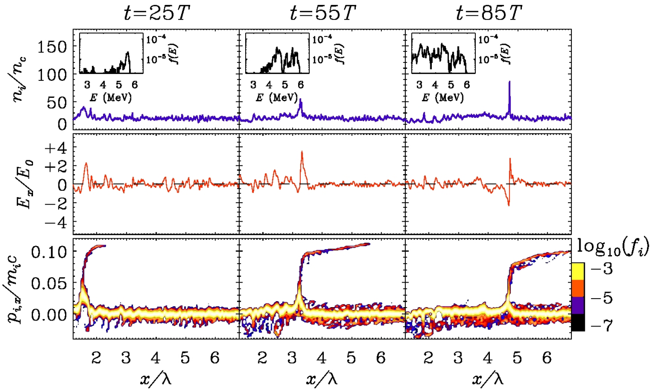

Too high T_i causes shock to slow down and spectrum to broaden

CSA with warm ions: 2D simulation (preliminary)

2D PIC simulation
laser pulse: $\tau_p = 45T$, $a_0 = 1$, $w = 5\lambda$
target: $n_e = 2n_c$, $T_i = 100$ eV, $Z/A = 1$

Same parameters as 1D (on axis) except lower resolution ($\Delta x = \lambda/100$, 100 part/cell)

CSA with warm ions: 2D simulation (preliminary)

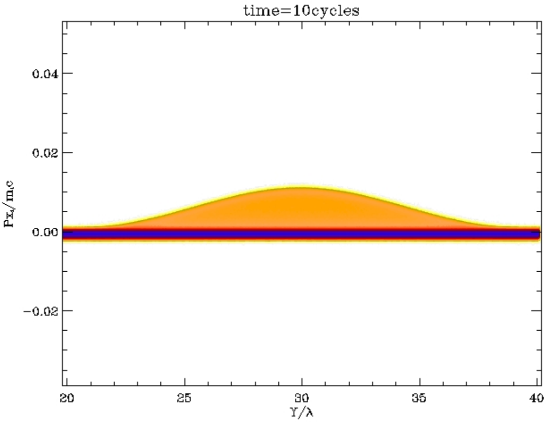

CSA with warm ions: 2D simulation (preliminary)

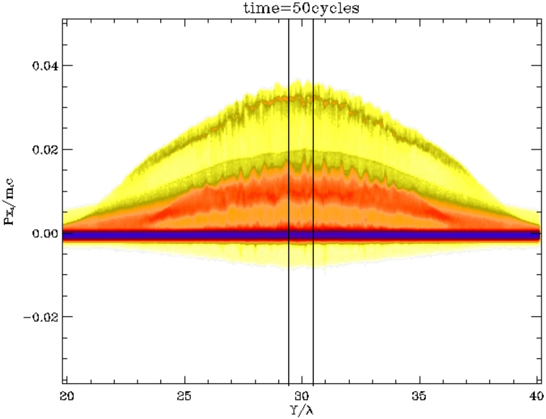

Ion spectrum near axis $29.4\lambda < y < 30.6\lambda$

Development of transverse "ripples"

CSA with warm ions: 2D simulation (preliminary)

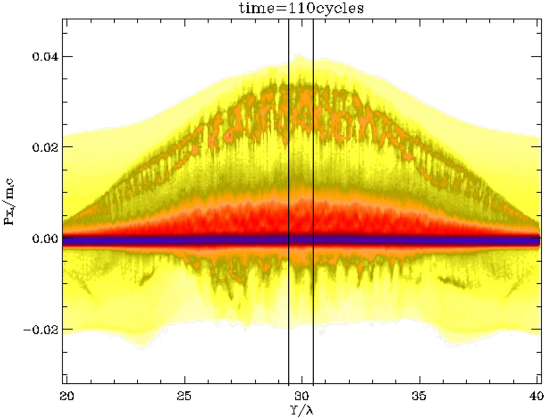

Ion spectrum near axis $29.4\lambda < y < 30.6\lambda$

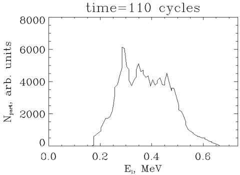

Reflected ions spectrum is much broader than in 1D

Promises and open issues with CSA

- Use of both gas laser and gas target is very suitable for high repetition rate
  (Gas jets with clusters seem also efficient with table-top optical lasers [Fukuda et al, PRL **103**, 165002 (2009)])
- Further theoretical investigation needed to understand shock front rippling and conditions for monoenergetic acceleration in 2D/3D
- More general issue: is it possible to have *both* efficiency and monoenergeticity in CSA?

Promises and open issues with CSA

- Use of both gas laser and gas target is very suitable for high repetition rate
  (Gas jets with clusters seem also efficient with table-top optical lasers [Fukuda et al, PRL **103**, 165002 (2009)])
- Further theoretical investigation needed to understand shock front rippling and conditions for monoenergetic acceleration in 2D/3D
- More general issue: is it possible to have *both* efficiency and monoenergeticity in CSA?

Promises and open issues with CSA

- Use of both gas laser and gas target is very suitable for high repetition rate
  (Gas jets with clusters seem also efficient with table-top optical lasers [Fukuda et al, PRL **103**, 165002 (2009)])
- Further theoretical investigation needed to understand shock front rippling and conditions for monoenergetic acceleration in 2D/3D
- More general issue: is it possible to have *both* efficiency and monoenergeticity in CSA?

Promises and open issues with CSA

- Use of both gas laser and gas target is very suitable for high repetition rate
  (Gas jets with clusters seem also efficient with table-top optical lasers [Fukuda et al, PRL **103**, 165002 (2009)])
- Further theoretical investigation needed to understand shock front rippling and conditions for monoenergetic acceleration in 2D/3D
- More general issue: is it possible to have *both* efficiency and monoenergeticity in CSA?

Promises and open issues with CSA

- Use of both gas laser and gas target is very suitable for high repetition rate

  (Gas jets with clusters seem also efficient with table-top optical lasers [Fukuda et al, PRL **103**, 165002 (2009)])
- Further theoretical investigation needed to understand shock front rippling and conditions for monoenergetic acceleration in 2D/3D
- More general issue: is it possible to have *both* efficiency and monoenergeticity in CSA?

TNSA: enhancing fast electron generation

TNSA is driven by *fast* electrons generated at the *front* surface of solid targets

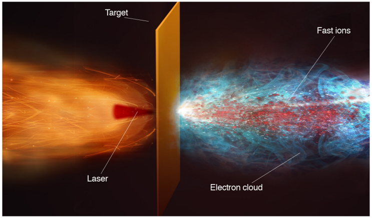

Key issue: increase conversion efficiency of laser energy in fast electrons

A strategy: special targets (mass-reduced, microstructured, low-density, . . .)

TNSA: enhancing fast electron generation

TNSA is driven by *fast* electrons generated at the *front* surface of solid targets

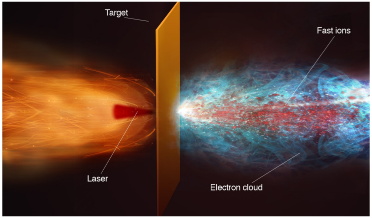

Key issue: increase conversion efficiency of laser energy in fast electrons

A strategy: special targets (mass-reduced, microstructured, low-density, . . .)

TNSA: enhancing fast electron generation

TNSA is driven by *fast* electrons generated at the *front* surface of solid targets

Key issue: increase conversion efficiency of laser energy in fast electrons

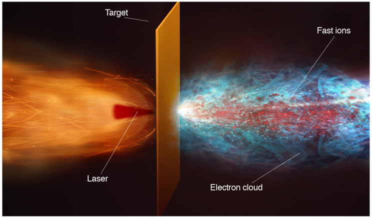

A strategy: special targets (mass-reduced, microstructured, low-density, . . .)

TNSA: enhancing fast electron generation

TNSA is driven by *fast* electrons generated at the *front* surface of solid targets

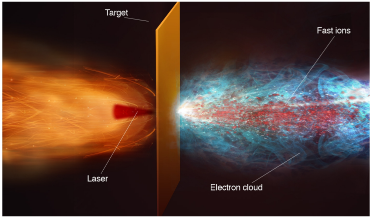

Key issue: increase conversion efficiency of laser energy in fast electrons

A strategy: special targets (mass-reduced, microstructured, low-density, . . .)

Enhanced TNSA in microcone targets

[Gaillard et al, Phys.Plasmas **18**, 056710 (2011)]
Experiment at TRIDENT, LANL (USA)

Use of cone target leads to
- effective grazing incidence
$\Longrightarrow$ more efficient
fast electron generation
- geometrical collimation of
fast electrons (“funnel” effect)

Up to 67.5 MeV protons observed with 80 J pulse energy

Enhanced TNSA in microcone targets

[Gaillard et al, Phys.Plasmas **18**, 056710 (2011)]
Experiment at TRIDENT, LANL (USA)

Use of cone target leads to
- effective grazing incidence
$\Longrightarrow$ more efficient
fast electron generation
- geometrical collimation of
fast electrons (“funnel” effect)

Up to 67.5 MeV protons observed with 80 J pulse energy

Enhanced TNSA in microcone targets

[Gaillard et al, Phys.Plasmas **18**, 056710 (2011)]
Experiment at TRIDENT, LANL (USA)

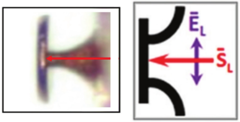

Use of cone target leads to
- effective grazing incidence
$\Longrightarrow$ more efficient
fast electron generation
- geometrical collimation of
fast electrons (“funnel” effect)

Up to 67.5 MeV protons observed with 80 J pulse energy

Enhanced TNSA in microcone targets

[Gaillard et al, Phys.Plasmas **18**, 056710 (2011)]
Experiment at TRIDENT, LANL (USA)

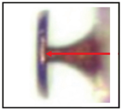

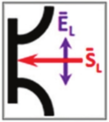

Use of cone target leads to
- effective grazing incidence
$\Longrightarrow$ more efficient
fast electron generation
- geometrical collimation of
fast electrons (“funnel” effect)

Up to 67.5 MeV protons observed with 80 J pulse energy

Enhanced TNSA in microcone targets

[Gaillard et al, Phys.Plasmas **18**, 056710 (2011)]
Experiment at TRIDENT, LANL (USA)

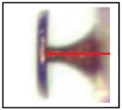

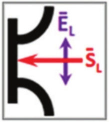

Use of cone target leads to
- effective grazing incidence
$\Longrightarrow$ more efficient
fast electron generation
- geometrical collimation of
fast electrons (“funnel” effect)

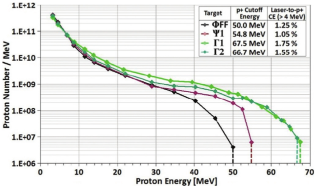

Up to 67.5 MeV protons observed with 80 J pulse energy

Enhanced TNSA in foam-covered targets

[Sgattoni, Londrillo, Macchi, Passoni,
PRE **85**, 036405 (2012)]

Self-generated channel
behaves similar to cone

$\mathscr{E}_{\mathrm{max}}$ doubles with foam
up to 15 MeV
in 3D simulation
with 1 J energy pulse

Enhanced TNSA in foam-covered targets

[Sgattoni, Londrillo, Macchi, Passoni, PRE **85**, 036405 (2012)]

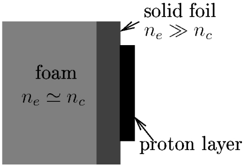

Self-generated channel behaves similar to cone

$\mathscr{E}_{\text{max}}$ doubles with foam up to 15 MeV in 3D simulation with 1 J energy pulse

Enhanced TNSA in foam-covered targets

[Sgattoni, Londrillo, Macchi, Passoni, PRE **85**, 036405 (2012)]

Self-generated channel behaves similar to cone

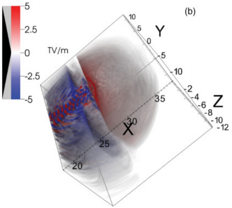

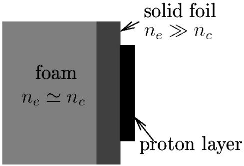

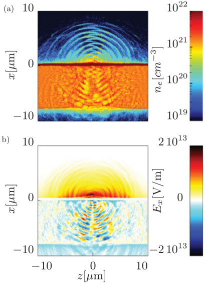

$\mathscr{E}_{max}$ doubles with foam up to 15 MeV in 3D simulation with 1 J energy pulse

Enhanced TNSA in foam-covered targets

[Sgattoni, Londrillo, Macchi, Passoni, PRE **85**, 036405 (2012)]

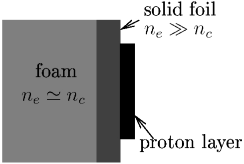

Self-generated channel behaves similar to cone

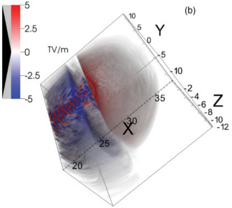

$\mathscr{E}_{\max}$ doubles with foam up to 15 MeV in 3D simulation with 1 J energy pulse

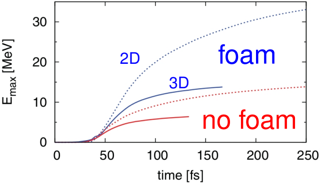

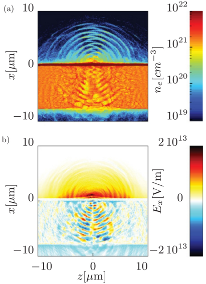

Foam-enhanced fast electron generation

2D parametric simulations:

Optimal foam mass density $n_e \ell$ exists
to enhance fast electron generation

fast electron temperature $T_f \gtrsim 3T_p$
where $T_p = m_e c^2 \left(\sqrt{1 + a_0^2/2} - 1 \right)$

P-component of $\mathbf{E}$
accelerates electrons
(coupling with
channel walls)

Remarkable similarity with cone-enhanced acceleration

Foam-enhanced fast electron generation

2D parametric simulations:
Optimal foam mass density $n_e \ell$ exists
to enhance fast electron generation

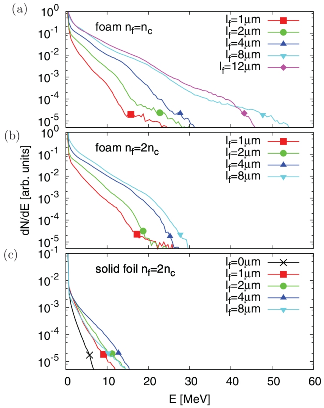

fast electron temperature $T_f \gtrsim 3T_p$
where $T_p = m_e c^2 \left(\sqrt{1 + a_0^2/2} - 1\right)$

P-component of $\mathbf{E}$
accelerates electrons
(coupling with
channel walls)

Remarkable similarity with cone-enhanced acceleration

Foam-enhanced fast electron generation

2D parametric simulations:
Optimal foam mass density $n_e\ell$ exists
to enhance fast electron generation

fast electron temperature $T_f \gtrsim 3T_p$
where $T_p = m_e c^2 \left(\sqrt{1 + a_0^2/2} - 1\right)$

P-component of $\mathbf{E}$
accelerates electrons
(coupling with
channel walls)
Remarkable similarity with cone-enhanced acceleration

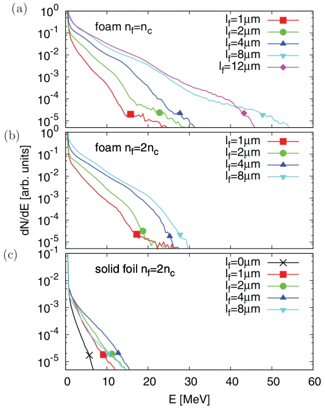

Foam-enhanced fast electron generation

2D parametric simulations:
Optimal foam mass density $n_e\ell$ exists
to enhance fast electron generation

fast electron temperature $T_f \gtrsim 3T_p$
where $T_p = m_e c^2\left(\sqrt{1+a_0^2/2}-1\right)$

P-component of $\mathbf{E}$
accelerates electrons
(coupling with
channel walls)

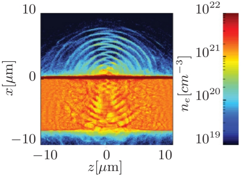

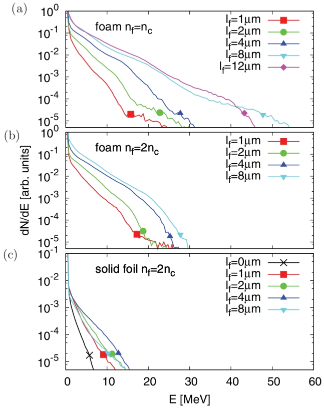

Remarkable similarity with cone-enhanced acceleration

Foam-enhanced fast electron generation

2D parametric simulations:
Optimal foam mass density $n_e\ell$ exists
to enhance fast electron generation

fast electron temperature $T_f \gtrsim 3T_p$
where $T_p = m_e c^2 \left(\sqrt{1 + a_0^2/2} - 1\right)$

P-component of $\mathbf{E}$
accelerates electrons
(coupling with
channel walls)

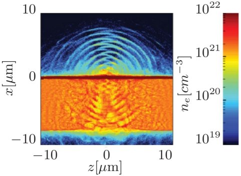

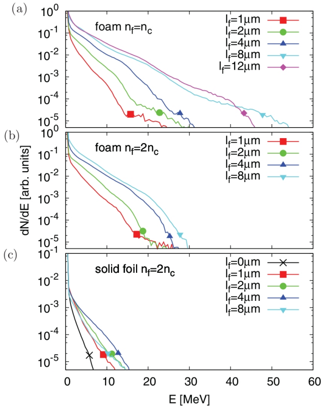

Remarkable similarity with cone-enhanced acceleration

Conclusions

RPA: Promising for acceleration to >1 GeV (with next term laser facilities)

$\longrightarrow$ need to improve spectrum, increase acceleration length, . . .

CSA: Attractive because of monoenergetic spectra and for gas-based scheme at high repetition

$\longrightarrow$ may be not efficient enough for applications

TNSA: Most tested mechanism, structured targets may increase energy and efficiency

$\longrightarrow$ need to improve spectrum and to check for high repetition rate operation

Conclusions

RPA: Promising for acceleration to >1 GeV (with next term laser facilities)

⟶ need to improve spectrum, increase acceleration length, . . .

CSA: Attractive because of monoenergetic spectra and for gas-based scheme at high repetition

⟶ may be not efficient enough for applications

TNSA: Most tested mechanism, structured targets may increase energy and efficiency

⟶ need to improve spectrum and to check for high repetition rate operation

Conclusions

RPA: Promising for acceleration to >1 GeV (with next term laser facilities)

$\longrightarrow$ need to improve spectrum, increase acceleration length, ...

CSA: Attractive because of monoenergetic spectra and for gas-based scheme at high repetition

$\longrightarrow$ may be not efficient enough for applications

TNSA: Most tested mechanism, structured targets may increase energy and efficiency

$\longrightarrow$ need to improve spectrum and to check for high repetition rate operation

Conclusions

RPA: Promising for acceleration to >1 GeV (with next term laser facilities)

$\longrightarrow$ need to improve spectrum, increase acceleration length, ...

CSA: Attractive because of monoenergetic spectra and for gas-based scheme at high repetition

$\longrightarrow$ may be not efficient enough for applications

TNSA: Most tested mechanism, structured targets may increase energy and efficiency

$\longrightarrow$ need to improve spectrum and to check for high repetition rate operation

Conclusions

RPA: Promising for acceleration to >1 GeV (with next term laser facilities)

$\longrightarrow$ need to improve spectrum, increase acceleration length, ...

CSA: Attractive because of monoenergetic spectra and for gas-based scheme at high repetition

$\longrightarrow$ may be not efficient enough for applications

TNSA: Most tested mechanism, structured targets may increase energy and efficiency

$\longrightarrow$ need to improve spectrum and to check for high repetition rate operation

Acknowledgments

- Work sponsored by the FIRB-MIUR (Italy) project SULDIS ("Superintense Ultrashort Laser-Driven Ion Sources")
- Use of supercomputing facilities at CINECA (Italy) sponsored by the ISCRA project TOFUSEX ("TOwards FUll-Scale simulations of laser-plasma EXperiments") award N.HP10A25JKT-2010